The processes dominating Ca dissolution of limestone when exposed to ambient atmospheric conditions as determined by comparing dissolution models

C. Cardell-Fernández · G. Vleugels · K. Torfs · R. Van Grieken

Abstract In order to gain a clearer understanding of the decay mechanisms operating in limestones, and to determine the main damage factors at different exposure environments, calcite-dissolution models from the literature were compared. The models recognise three major stone decay mechanisms: attack by air pollutants (dry deposition), dissolution in clean rain (karst effect) and dissolution caused by neutralisation of rain acidity (acidity effect). These models were fitted to experimental data obtained from the run-off water analysis running over the so-called Massangis limestone, exposed under ambient conditions in five sites in Belgium. The models demonstrate that different processes dominate the limestone dissolution at the different sites, with dry deposition of air pollutants (especially SO_2) being the principal process involved.

Keywords Acidity effect · Dry deposition · Karst effect · Limestone material loss · Massangis limestone (northern France)

Introduction

The erosion rates of building stones can be studied on a quantitative base by analysing water runoff at frequent time intervals. That is, the rainwater that has run over a well-defined area of a building wall, or over a stone slab that is exposed to ambient atmospheric conditions (Cooper 1986; Livingston 1992; O'Brien and others 1995; Torfs and Van Grieken 1996; Sweevers and others 1998, unpublished data). When rainwater interacts with a stone surface, ions are exchanged: the stone either loses ions by dissolution or it retains ions contained in the rainwater. To determine recession rates, this study focused on stone material loss. Because the amount of calcium in the water run-off is a measure of the dissolution and removal of calcium carbonate from the limestone surface, the net calcium loss in the water run-off is used to determine stone weathering (Sherwood and Reddy 1988). Material loss from carbonate stones that are exposed over a long period may be mainly a result of chemical attack, but also because of physical factors such as flaking, abrasion and cracking; whereas fresh limestones mostly loose material by chemical dissolution, particularly on rain-washed stones (Webb and others 1992). A direct estimate of the total mass released from a limestone during the process of rainwater running over its surface can be provided by the combination of microcatchment units (MCUs) and sensitive analytical methods (Livingston 1986; Reddy 1988). To quantify the effects of factors that control stone decay, several damage functions have been proposed for limestones based on insights into the dissolution process and/or linear regression fits to large, experimentally obtained data sets (Lipfert 1989; Baedecker and others 1992; Butlin and others 1992; Kucera and Fitz 1995). These functions aim to predict overall stone loss caused by interactions with the rainwater. The goal of this paper was to make a comparison between four calcium dissolution models proposed in the literature, namely those of Livingston (1992, unpublished data), Lipfert (1989), Webb and others (1992) and Baedecker and others (1992). Each model attempts to accurately specify the course of dissolution in limestones and to estimate the relative importance of different dissolution processes. The models permit us to predict the material loss by rain-wash. The four models selected in this work were fitted to a huge experimental data set obtained from a limestone-exposure programme in Belgium (involving data from the analysis of 3,000 water run-off samples), and their performances were compared.

Received: 20 June 2000 / Accepted: 9 June 2002
Published online: 7 August 2002

C. Cardell-Fernández · G. Vleugels · K. Torfs
R. Van Grieken (✉)
Department of Chemistry,
University of Antwerp (UIA),
Universiteitsplein 1, Antwerp, Belgium
E-mail: vgrieken@uia.ac.be
Tel.: +32-3-8202362
Fax: +32-3-8202376

 DOI 10.1007/s00254-002-0640-x

Material, experimental design and measurements

Massangis limestone

Massangis limestone was selected for this study because of its importance in the restoration of historic buildings in Western Europe. The outcrop is located in the village of Massangis, approximately 22 km north of Avallon (Northern France). Currently, the only quarry in production is "Les Pelottes", sited 1.5 km west of the village. The Massangis limestone was formed at the Bathonian stage (Middle Jurassic). It is an oolitic limestone containing some shell fragments and occasional nodules of siliceous or pyritised materials. The lithotype under study belongs to a variety known as "Roche Jaune" with a characteristic deep yellow to brown coloration. This limestone is composed mainly of calcite (>98%) and small amounts of iron and magnesium. Larger fragments of brachiopod shells (<8 mm) and also crinoids are observed. The scarce cement is sparitic. The variation in grain size is quite wide (1.5–100 μm) and its porosity, mostly intergranular, ranges between 8 and 15% in volume, with a mean porosity of 13.6% (Dickinson and others, unpublished data). The chemical composition of the fresh limestone (Table 1) was determined previously by laboratory experiments with energy dispersive X-ray fluorescence spectrometry (ED-XRF) and neutron activation analysis (NAA). In addition, mineralogy and texture were examined by optical microscopy. After undergoing decay, stone slabs, prepared as thin sections, were analysed by electron probe X-ray microanalysis (EPXMA) and photo-acoustic Fourier transform infrared spectrometry (PAS-FTIR) to compare the exposed surfaces of the stone samples with fresh inner surfaces. These results are reported in Vleugels (unpublished data).

Sampling device

A set of samples were exposed in so-called "microcatchment units" (MCUs) to quantify the material loss of the limestones. In the MCUs (Jeffrey and others 1985), a 25×25-cm stone slab (5 cm thick) was held in a glass holder, cemented on top of a polystyrene box, filled with gravel and exposed at an angle of 15° to minimise splash/blow-out losses (Fig. 1). The incident rainfall struck the surface and ran over the inclined stone into a polystyrene tube and was collected in a bottle for analysis. A chemically inert roughened glass surface of identical dimensions as the exposed stone area was used as a blank reference system. The MCUs were oriented to the prevailing rain and wind direction (SW) and exposed for 3 years at five sites in Belgium: the Antwerp University Campus (UIA); near a busy street in the centre of Antwerp (PML); the industrial harbour area of Antwerp, close to many large chemical and petrochemical plants (PORT); a small village at the Belgian North Sea shore (SEA) and a remote location in the Ardennes hills in southern Belgium (OFF). In each Belgian monitoring site, two stone slabs were exposed together

Table 1
XRF-bulk analysis (ppm) of fresh Massangis limestone. K, Ca and Fe are expressed in %

Na	K	Ca	Ti	Mn	Cr	Fe	Cu	Ni	Zn	Ba	Rb	Sr
190	0.40	47	40	37	8.4	0.25	2.5	30	13	<30	10	242
Zr	Sc	Cr	Co	As	Se	Br	Mo	Ag	Sb	Cs	La	Ce
12	0.41	6.2	0.28	0.55	<6	2.75	<4	<0.2	<0.2	0.55	2.25	2.15
Nd	Sm	Eu	Tb	Dy	Ho	Tm	Yb	Lu	Hf	Ta	W	Hg
<5	0.36	0.06	<0.1	<3	<0.3	0.11	0.24	0.04	0.05	<0.1	<0.6	<0.2
Th	U											
0.23	0.50											

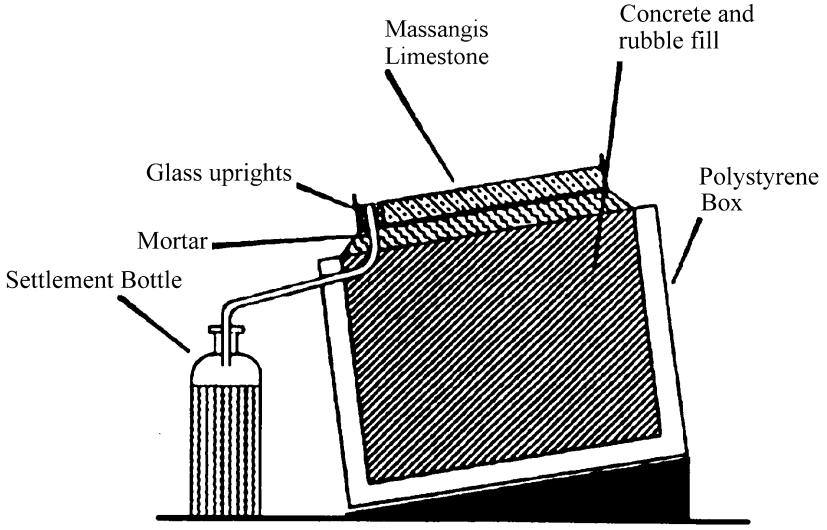

Fig. 1
Schematic representation of a "microcatchment unit" (MCU)

with two blanks in MCUs. The run-off water was sampled at weekly or two-weekly intervals (depending on the rain volume) over a period of 3 years. Around 3,000 samples were analysed during these field experiments.
Together with the sample collection, environmental data were continuously collected from governmental organisations. The Belgian Institute for Hygiene and Epidemiology, which operated the Automated Network for Pollution Monitoring (unpublished data), supplied the dust and pollution data (SO_2, NO, NO_2, C_nH_m, O_3). The meteorological parameters (temperature, relative humidity, rainfall amount, rain intensity, wind speed and direction, number of freeze–thaw cycles, and number of days with snow, storm and hail) were provided by the Royal Meteorological Institute (unpublished data). More than 5,000 meteorological and atmospheric data conditions were gathered at the sampling sites. The average environmental conditions at the exposure sites are shown in Table 2. A high SO_2 level (around 60 μg m^{-3}) was found at the PORT, as was expected considering its location in the industrial harbour area. The UIA and PML sites are strongly influenced by urban and industrial environments with SO_2 levels of around 30 μg m^{-3}. In addition, the PML location has the higher levels of NO and NO_2 (both around 55 μg m^{-3}). The SEA and OFF sites can be characterised, from the pollutant levels, as background sites; they are the only ones where O_3 was detected (values of 38 and 46 μg m^{-3}, respectively). Most of the pollution data were obtained by half-hour measurements. The heaviest rainfall occurs at the SEA and the PML sites, and the lowest at the OFF and UIA sites, with fluctuating levels of between 0.9 and 1.1 l m^{-2} day^{-1}. The relative humidity is quite high at all sites (75–81%), but especially at the coastal areas. The lower temperatures and the higher number of freeze–thaw cycles, and days of snow and hail were measured at the OFF site. Similar average wind speeds, with a range of 15 and 20 km h^{-1}, were detected for all locations, except the SEA site, which had stronger winds.

Analytical methods

The volume of the run-off samples was determined and, later, the solutions were filtered through a 0.22-μm pore-size Millipore filter. The mass of the total suspended particulate matter (TSP) was established by weighing the filters before and after filtration. The nature of the TSP in the run-off water was automatically analysed by EPXMA on a particle-by-particle basis, and classified according to their chemical composition using a JEOL JXA-733 electron probe X-ray microanalyser equipped with a Tractor Northern TN-2000 energy-dispersive X-ray detection system. The concentrations of the ions, characteristic for the building stones, and those related to air pollution, were analysed in the water run-off samples. pH was determined as soon as possible, generally within a day, by means of a combined glass electrode and potentiometry. Water samples were then stored in a refrigerator prior to further analyses for major ions. The HCO_3^- content was analysed by titration using HCl on a methyl orange indicator. Ion chromatography (IC) was used to determine Cl^-, NO_3^- and SO_4^{2-} by means of a Dionex 4000i equipped with an AS4A separator column. Na^+ and K^+ were measured by atomic emission spectrometry (AES), and Mg^{2+} and Ca^{2+} were assessed using atomic absorption spectrometry (AAS), both with a Perkin–Elmer 3030 spectrometer. A complete description of the sampling sites, experimental procedure and data can be found in Vleugels and Van Grieken (1995).

Table 2
Average environmental conditions at the five exposure sites in Belgium

	SO_2 (μg m^{-3})	NO_2 (μg m^{-3})	T (°C)	Rain (mm $year^{-1}$)	Rain (pH)
UIA	29	30	9.5	700	3.6
PML	27	55	11	650	3.7
PORT	59	49	11.5	750	3.7
SEA	9	20	10	650	4.4
OFF	12	12	7	950	4.5

Limestone dissolution processes

Acid rain and dry deposition of SO_2 cause dissolution of carbonaceous stones, which results in material loss. Dry SO_2 deposition comes primarily from local pollution sources, whereas acid rain can result from long-range transport from diverse pollution sources. For purposes of developing air-pollution control policies to protect architectural monuments, it is important to distinguish between both processes. To investigate this matter, run-off experiments are commonly used. However, the natural dissolution of limestones in clean, unacidified rain, which is called the karst effect, must also be taken into account. Theoretical models concerning the chemical dissolution of rain-washed limestones have been derived from considerations of the ion and mass balances between the incident rain and the run-off water. Similarly, theoretical equations for chemical dissolution of calcareous stones generally recognise three mechanisms for material loss (Benarie 1991): (1) attack by gaseous pollutants, mainly SO_2, with subsequent $CaSO_4{\cdot}2H_2O$ precipitation and dissolution, (2) dissolution in clean rain because of interaction with water and CO_2, or the so-called karst effect, and (3) dissolution caused by neutralisation of excess rain acidity from air pollution. The total material loss of a limestone because of dissolution during an exposure period is the sum of these three terms for each rain event (Webb and others 1992). Thus, according to Livingston (unpublished data), by using data transformations based on electrolyte theory and the carbonate equilibrium, the total observed dissolution of calcium from a calcareous stone can be partitioned into components of natural or karstic dissolution, dry deposition (dissolution caused by gaseous pollutant reaction) and wet deposition of pollutants (dissolution due to acid rain or acidity effect). According to this author, the estimated material loss from the composition of the dissolved phase of the run-off water is specifically referred to as denudation, to distinguish it from other quantitative measurements of weathering.

Karst effect

The karst effect concerns the natural dissolution of limestones by rainwater, which normally is only acidified by CO_2 or organic acids, as compared to mineral acids. Limestones are slightly soluble in rainwater because calcite is slightly soluble in pure water, although the solubility increases in the presence of CO_2. This process should not be ignored even when acid rain is present. The term is introduced to distinguish between the natural rates of weathering and those due to man-made acidity in the rain, represented principally by H_2SO_4 and HNO_3. The dissolution of calcite is more complex than that of gypsum because it affects the dissolution equilibrium of carbonates. Karst dissolution, or dissolution in absence of mineral acids, is described as:

$$CaCO_3 + H_2O + CO_2 \Leftrightarrow Ca(HCO_3)_2 \quad (1)$$

Calcium bicarbonate is about a hundred times more soluble (1.1 g l^{-1}) than calcium carbonate (1.4×10^{-2} g l^{-1}). The excess bicarbonate produced by the stone dissolution reacts with H^+ and forms carbonic acid:

$$H^+ + HCO_3^- \Leftrightarrow H_2CO_3 \quad (2)$$

In an open system where solution and stone are exposed to the atmosphere, the resulting excess of carbonate disturbs the equilibrium, as shown in the following equation, which is restored by the liberation of CO_2 gas:

$$H_2CO_3 \Leftrightarrow H_2O + CO_2 \uparrow \quad (3)$$

Hence, the dissolution of calcite is always associated with an increase in pH. Nevertheless, an upper limit exists, which is determined by the atmospheric CO_2 level.

Dry deposition

Dry deposition takes place between precipitation events; however, some moisture in the stone surface is required for the reaction to proceed. The end result of the dry deposition processes is predominantly the formation of gypsum, which has a much higher solubility than calcite. Dissolution of gypsum is quite simple:

$$CaSO_4 \cdot 2H_2O \Leftrightarrow Ca^{2+} + SO_4^{2-} + 2H_2O \quad (4)$$

During this reaction, no shift in pH or HCO_3^- concentration occurs, but a net gain in SO_4^{2-} concentration is obtained. As there is no source of sulphur in the stone, any increase in SO_4^{2-} between the rainfall and the run-off water is attributed to gypsum formed during dry periods by the attack of sulphur dioxide. The dissolution of gypsum does not influence the pH or the carbonate dissolution equilibrium.

Acidity effect

Acid rain is defined as the presence of acidity in rainwater in excess of naturally present acids. This anthropogenic contribution consists mainly of H_2SO_4 and a smaller and more variable amount of HNO_3. When acid rain reaches the limestone surface, it is neutralised:

$$CaCO_3 + 2H^+ + SO_4^{2-} \Leftrightarrow Ca^{2+} + H_2O + CO_2 \uparrow + SO_4^{2-} \quad (6)$$

It should be remarked that the SO_4^{2-} (or NO_3^-) concentration in rain does not change during the neutralisation process. The most significant effect of this reaction is the pH increment. In addition, this reaction indirectly affects the HCO_3^- concentration through the equilibrium of carbonate species in the solution with atmospheric CO_2.

Theoretical models for limestone dissolution

For the purpose of this work, four theoretical calcite dissolution models from the literature, with similar bases but different elaboration, have been selected and compared.

The Livingston model

Livingston (unpublished data) pointed out that, using the electrolyte theory and carbonate equilibria, it was possible to derive a mathematical model that uses ionic changes to evaluate the relative impact of the different above-mentioned processes on the overall dissolution rate of carbonate stones. The increase of calcium in the run-off is the sum of three different reactions, namely acid rain, dry deposition and karst dissolution. Each represents a different weathering process and produces its own characteristic changes in SO_4^{2-}, H^+ and HCO_3^- concentrations.

The author remarks that prior to carrying out any regression analysis, it is essential to study the total calcium loss data for visual interpretation; for instance, plotting it by means of triaxial diagrams, which supply an index of the relative importance of the three carbonate dissolution processes (Livingston 1992). But this method does not provide an estimate of the actual magnitude of the amount of dissolved carbonate stone. More information can be obtained from the reaction paths/phase diagrams, by plotting the pairs of rainfall/run-off data on a diagram with axes of [Alk], which is the alkalinity, and $[SO_4^{2-}]$. This is because the carbonate dissolution model can be written as a linear combination of these two variables:

$$\Delta\left[Ca^{2+}\right] = 0.5\Delta[\mathrm{Alk}] + \Delta\left[SO_4^{2-}\right]$$

where:

$$[\mathrm{Alk}] \equiv \left[HCO_3^-\right] + 2\left[CO_3^{2-}\right] + \left[OH^-\right] - \left[H^+\right]$$

Any point on the [Alk]–[SO_4^{2-}] plane represents a unique value of [Ca^{2+}], and the distance between a pair of points is a measure of $\Delta[Ca^{2+}]$. The author proposes that $\Delta[Ca^{2+}]$ is not simply a linear function of $[H^+]_{rain}$, as was assumed by Reddy (1988) in linear regression analyses. Because the precision of the chemical analysis of calcium in solution

can be in the range of calcium in the run-off (due to acid rain), some acid rain indicators in the data may be lost in the noise.
The equation for the dissolution model proposed by Livingston is:

$$\Delta[Ca^{2+}] = \Delta[SO_4^{2-}] + 10^{-11.6}\left(\frac{1}{\gamma_{runoff}[H^+]_{runoff}} - \frac{1}{\gamma_0[H^+]_0}\right) - 0.5\left([H^+]_{runoff} - [H^+]_0\right) + 10^{-11.6} \times \left(\frac{1}{\gamma_0[H^+]_0} - \frac{1}{[H^+]_{rain}}\right) - 0.5\left([H^+]_0 - [H^+]_{rain}\right)$$

where $\Delta[Ca^{2+}]$, $\Delta[SO_4{}^{2-}]$ are calcium and sulphate concentration change in the rainwater before and after reaction with stone (mol l^{-1}); $[H^+]_0$ is the H^+ concentration in rain in the absence of anthropogenic contributions ($=10^{-5.6}$ mol l^{-1}); γ is the activity coefficient in the run-off; and γ_0 is the activity coefficient in rain in the absence of anthropogenic contributions.
The first term in the equation describes the dry SO_2 deposition effect, the second and the third terms describe the karst effect, and the fourth and the fifth terms are the wet acid deposition. The contribution of the excess acid rain to the total calcium loss from the stone is determined by the blank pH, which can be as low as 3.5 in the present work. The pH of the stone run-off water is predominant in karst dissolution. This implies that it is not possible to predict the amount of calcite dissolution simply from the observation of rainfall pH. The run-off pH, which is determined by flow conditions over and through the stone and varies from one event to the other, must be known (Livingston 1986). One shortcoming of the Livingston model is that it only predicts dissolved material loss and neglects suspended particulate matter. In addition, it uses concentration units whereas amounts are required for an exact calculation of net loss.

The Lipfert model

Lipfert (1989) reviewed the results from 15 stone-loss experimental programmes and then used regression analysis to postulate (but he did not fully derive) a theoretically-based damage function for a generic calcite, based on dry deposition, karst effect and acidity effect.
The equation he proposed is:

Stone loss (μm per m of rain)

$$= 18.8 + 0.016H^+ 0.18[v_d \cdot C_{SO_2}]/\text{rain}$$

where H^+ is the concentration of acidity (mmol l^{-1}); v_d is the deposition velocity (cm s^{-1}); C_{SO2} is the measured as a air concentration (μg m^{-3}); and rain is measured in m.
This damage function is based on the solubility of calcite in equilibrium with a P_{CO2}=330 ppm, and is valid for a precipitation pH in the range of 3–5. The intercept term, which can be interpreted as an indication of an incomplete regression, has a value of 18.8 in this equation. The second term denotes the acceleration of dissolution caused by rain acidity. The last term indicates the attack by gaseous pollutants, assuming that each deposited molecule of SO_2 will react with one molecule of $CaCO_3$. A disadvantage of this model is the tendency to exaggerate the karst effect, by assuming that the run-off water always reaches saturation with respect to calcite.
In Lipfert's summary, only nine of the reviewed studies include measurements of environmental variables (as for instance that of Reddy and others 1985). Those that do include the measurements, incorporate values for both the acid deposition and the sulphur dioxide concentration and, thus, permit the examination of cause–effect relationships. Of these experimental programmes, only two studies enclose data on incident rainfall pH or amounts. The remaining seven studies relate stone weathering only to sulphur dioxide air concentrations or deposition. As a result, the proposed theoretical equation by Lipfert does not consider either the variation in the ratio of the rainfall interception and the total exposure areas of the stone samples between different studies, or the possible variations of evaporation rates in the stones. The former parameter could be important for great differences in sample geometry and exposure positions, whereas variations in evaporation have probably more influence in studies carried out in quite different climates using stones with different porosities. In addition, this model also considers the stone loss in concentration units because the data are compiled and compared on the basis of material loss per meter of incident precipitation (concentration units).

The Webb model

Webb and collaborators (1992) derived a theoretical damage function by considering the chemical dissolution of rain-washed limestones. The model was fitted to the experimental data from nine field test sites in England and Scotland, for a period up to 3 years, by adjusting the system variables within physical realistic limits. They put forward the following equation:

Stone loss (mol)

$$\cong \text{ADV}_d C_{SO_2} + \frac{K_H K_1 P_{CO_2}}{2[H^+]_r}\Sigma(A_i R - \text{Evap}) + \frac{[H^+]_i}{2}\Sigma A_i R$$

where A is the surface area of the stone exposed (m^2); V_d is the dry deposition velocity (mm s^{-1}); C_{SO2} is the mean SO_2 concentration (μg m^{-3}) during the exposure of duration D (s); A_i is the rainfall interception area (m^2); R is the intercepted rainfall (mm); $[H^+]_r$ is the volume-weighed mean H^+ concentration of the run-off (mol l^{-1}); $[H^+]_i$ is the volume-weighed mean H^+ concentration of the total deposition (mol l^{-1}); Evap is the volume of rainfall evaporated from the stone sample (mm); and K_H, K_1 are the equilibrium constants for Eqs. (3) and (2), respectively, after Stumm and Morgan (1970); P_{CO2}: 350 ppm.
As run-off and the incident rain volumes were measured in this study, the equation can be simplified to:

$$\text{Stone loss (mol)} \approx \text{ADV}_d C_{SO_2} + \frac{K_H K_1 P_{CO_2}}{2[H^+]_r} \Sigma_{\text{volume}_r} + \frac{[H^+]_i}{2} \Sigma_{\text{volume}_i}$$

where $volume_r$ volume of the run-off solution, and $volume_i$ volume of the total deposition. The first term in both equations stands for the dry deposition effect. The second term describes the karst dissolution, and the third gives the rain acidity neutralisation. Several advantages can be reported for this method. Thus, the authors considered the effects of wind speed, humidity and time of stone wetness to study the variations in the dry deposition velocity between sites, concluding that the inter-exposure variations were not a very important factor in stone loss. The SO_2 concentrations in air were measured continuously by ultraviolet fluorescent and chemiluminescent analysers in all monitored sites. In addition, the daily temperature data were available for the sampling programmes, so the $K_H K_1$ product in the formula can be treated as a constant depending on the temperature ($K_H K_1 P_{CO2}=1.8\times10^{-10}$). Among the shortcomings of the proposed dissolution model, it should be mentioned that the variation in run-off pH with rainfall intensity and the rainfall interception between rain events and between sites (which could improve the quantitative and predictive capabilities of the model) are not considered. Thus, the authors use a typical pH of around 4.5 for rainwater in United Kingdom, with the run-off water from limestone having a pH ranging of 7–9. In addition, they ignore the possible influence of salt accumulated in the stone, and the granular loss of material resulting either by physical processes or from preferential dissolution of the cementing calcite. Webb and collaborators concluded that the variation between the calculated stone loss from their model and the measured mean loss rate for any exposure is generally smaller than the variation between the triplicate samples.

The Baedecker method

This is a graphical method (Baedecker and others 1992) where the cumulative amount of Ca^{2+} removed from the stone surface, the cumulative excess of H^+, and sulphate and nitrate (blank corrected and therefore dry deposited) in the run-off solutions, are plotted against either the cumulative volume of run-off solution or the exposure time. The relative contribution of the mentioned effects is calculated from the endpoint in the cumulative plots. Baedecker and collaborators assign the differences between the cumulative H^+ deposited as the karst effect ("clean rain" solubility of the stone):

$$\text{Karst} = Ca^{2+}\text{loss} - \left(SO_4^{2-}\text{loss} + NO_3^-\text{loss} + H^+\text{input}\right)$$

$$\text{acid} = H^+\text{input}$$

$$SO_2 = SO_4^{2-}\text{loss}$$

The contribution of the karst effect can be calculated from the cumulative excess of HCO_3^- in the run-off water:

$$\text{Karst} = HCO_3^-\text{loss}$$

As a result, less than 100% of the calcium loss is explained when other processes other than these three are involved. This graphical method has the advantage that it estimates and compares both chemical and physical erosion. Physical erosion measurements were obtained from gravimetry and interferometry to evaluate the importance of grain loss to the total erosion process, plus supplementary data of chemical composition of suspended particulate matter in run-off experiments. Also, the authors considered the effect of rain interception on the stone erosion surface (for example droplet size, retention of water by the stone and wind speed), which is important for evaluating the relative contribution of wet and dry deposition to carbonate stone erosion and for using the carbonate equilibria. Among the shortcomings, they simplify the dissolution model ignoring the alkalinity (or pH) of both rainfall and run-off water. In addition, although the SO_4^{2-} and NO_3^- concentrations were corrected for the ambient levels of SO_4^{2-} and NO_3^- in the rain, as well as the contribution of the same anions through dry particle deposition (by subtracting the concentrations observed in the blanks for each collection period), the effect of dry deposition on the stone surface can be underestimated by assuming that dry gaseous deposition in the blank is negligible.

Results and discussion

Material loss

As has been mentioned, based on the run-off chemical analysis and, more particularly, the ion-exchange between rainwater and run-off resulting from the interaction of the rain with the stone surface, the material loss for calcareous stone can be quantified. In this study, net ion-exchanges were calculated for the selected ionic species from the stones located at the different collection sites by subtracting the amount of each ion in the blank sample from the amount measured in the stone run-off water. By adding successive amounts, cumulative net ion-exchanges were obtained. Analytical data of the blank and run-off waters, averaged over two identical samples, and the meteorological variables and pollutant parameters recorded in Belgium during the period of this work, are shown in Vleugles (1992). The data were collected at least in duplicate at each station. The pH of the limestone run-off water was generally in the range of 6–8, which was on average 2 units higher than that of the blank samples. Ionic concentrations were generally higher than those measured in the blank samples.

Any enrichment in ion concentration between the blank and the stone run-off water is attributed to material lost from the stone surface (Livingston 1986). Often, the released ions are calculated by multiplying the run-off volume by the ion concentrations, although the use of amounts instead of concentrations permits a more correct estimation of the real calcareous stone loss (Steiger and Dannecker 1994). Thus, the Ca^{2+} loss can be referred to as

a function of the other ions lost by the stone expressed as μ eq mcu^{-1} $week^{-1}$. The net Ca^{2+} loss in the run-off water is used to determine stone weathering because the amount of Ca^{2+} in the run-off water is an indicator of the dissolution and removal of calcium carbonate from the limestone surface (Sherwood and Reddy 1988). Nevertheless, material loss calculated from run-off chemistry is preferably expressed in units of mass $area^{-1}$ $time^{-1}$. However, even when "mass" loss data are obtained, as in the case of microcatchment units, the results generally are expressed in the literature in the units of length/time (Livingston 1986). The erosion rate is determined by recalculating the material loss per year, namely μm $year^{-1}$. As the processes involved in stone erosion display a rain dependence, it is convenient to express stone decay in terms of material loss per meter of incident rainfall (Lipfert 1989).

Usually, the material loss rate is calculated from the dissolved material only, neglecting the non-dissolved matter. Although, as Roekens and Van Grieken (1989) and Vleugels and Van Grieken (1995) have mentioned, the suspended particulate matter may contribute 50% on average to the total material loss of a historic limestone building. The surface recession rates of the Massangis limestone were derived by regressing the net Ca^{2+} dissolved in the run-off water plus the total suspended particulate matter (TSP), versus the ionic input to the stone (= blank) and versus meteorological and atmospheric parameters acting on the limestone. Principal component analysis (PCA) and factor analysis (FA) were used to interpret the relationships between the variables (analytical data of rainwater samples and meteorological data) and to predict the stone loss. PCA is a statistical technique to reduce the dimensionality of a large data set through transformation of the original correlated variables into new uncorrelated variables, the principal components, which are linear combinations of the original data set and are deduced in descending importance. A principal component is composed of the product of a loading vector and a score vector plus an error term. The loadings represent the cosines of the angle between the original variables and the new components. PCA analyses were performed with the software program Unscrambler 3.54 (Tysso and others 1987). Later on, the data were evaluated with FA using IDAS software (Bondarenko and others 1995).

The average annual material loss of the exposed Massangis limestones is shown in Fig. 2, which indicates the relative contributions of the dissolved $CaCO_3$ and the total suspended particulate matter loss. Rate of loss clearly differs between the five sites. Massangis limestone erodes at an average rate of 12–14 μm m^{-1} of incident rainfall, over an initial 3–4-year period of exposure in Belgium. The relatively high TSP load in the run-off water for the limestones in the industrial harbour area of Antwerp (PORT) is interpreted to be caused by the supersaturation of the solution because of the intense release of ions from the stone. The relatively high TSP loss in the UIA site is ascribed to a similar process; for instance, because of the abrasion of the stone surface by rainfall or wind erosion effects. The rate of erosion caused by mechanical removal of granular

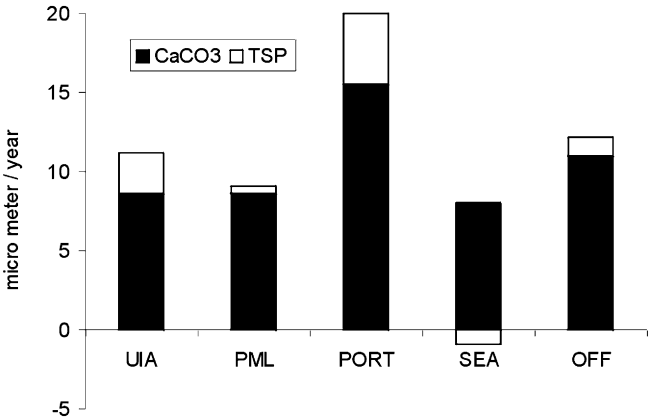

Fig. 2
Relative contributions of annual material losses of exposed Massangis stones calculated from dissolved Ca^{2+} (as $CaCO_3$) and TSP (total suspended particulate matter)

material from the stone surface by, for example, high rainfall, can exceed the rate of stone loss by dissolution by nearly a factor of three for limestones, according to Baedecker and others (1992). The marked wetness surface of the limestones at the seaside sites, favoured by the high relative humidity and presence of hygroscopic sea salts, enhances the uptake and retention of particles by wet and dry deposition, rather than material loss. Nearby buildings may also alter the local conditions at PML (centre of Antwerp), by enhancing the relative humidity, which reduces the particulate loss from stones. As Steiger and Dannecker (1994) have suggested, the net input of a stone strongly depends on the interaction of many different parameters, among others, the chemical composition and intensity of the rain, the ambient concentrations of gases and particulate pollutants, and the properties of the stone material with respect to water uptake (rate of infiltration). For all sites, the $CaCO_3$ + TSP loss is well correlated with the run-off water volume, but less with the rain amount. In addition, a correlation of the $CaCO_3$ + TSP loss with the deposition velocity of SO_2 was observed for the PORT samples, and with wind speed for the UIA site. For the Massangis limestones exposed at the five monitoring sites in Belgium, a good correlation was found between the average annual mean SO_2 level in the ambient and the corresponding annual mean of $CaCO_3$ + TSP (Fig. 3). The correlation matrices of the ion-exchange amounts (meq $catchment^{-1}$) averaged over two Massangis stones, and the meteorological and air quality parameters for each of the five sites separately can be found in Vleugels (1992).

Fitting of experimental data to theoretical models for calcium dissolution

The already mentioned four theoretical models for calcium dissolution in limestones were used to provide estimates of the contribution to calcium loss of: dry SO_2 deposition, karst dissolution effect and wet acidity deposition. The results are as follows

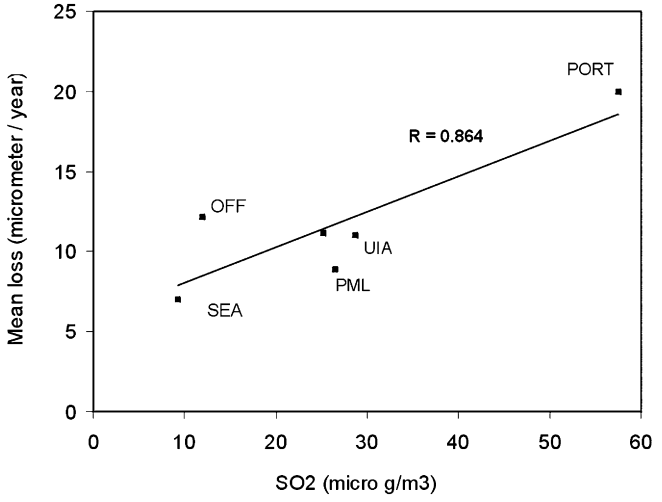

Fig. 3
Correlation between the annual mean ambient SO_2 level at five sites in Belgium, and the corresponding mean annual $CaCO_3$ + TSP loss from Massangis stones

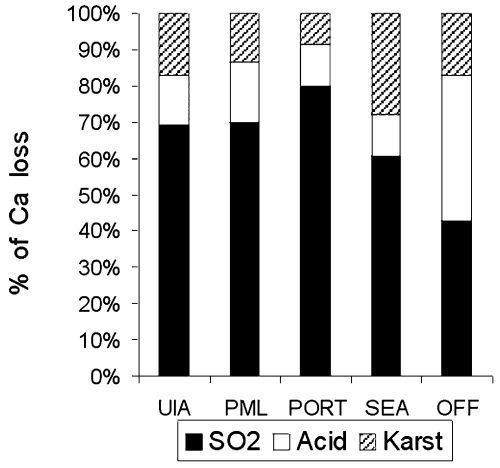

Fig. 4
Relative contributions of the three processes (rain acidity, dry deposition of SO_2 and natural dissolution) to calcium loss from Massangis limestone using the Livingston model

The Livingston model

The total calcium loss by the limestones is the sum of the three derived terms: dry deposition, acid rain and karst effect, and can be described as:

$$\Delta\left[Ca^{2+}\right] = \Delta\left[SO_4^{2-}\right] - \frac{\Delta[H^+]}{2}\left(1 + \frac{10^{-11.3}}{[H^+]_{blank}[H^+]_{stone}}\right)$$

The relative contributions of the three processes to calcium loss are illustrated in Fig. 4. The bars were obtained by applying the model to the mean values of the ionic concentrations. The contribution of acid rain excess to total calcium loss of the stone was determined by the blank pH, instead of rain concentrations. The contribution of dry deposition of SO_2 appears to be the most important weathering factor for the Massangis limestones in the area

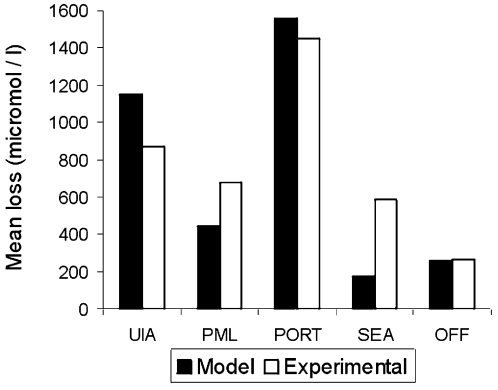

Fig. 5
Comparison of experimentally obtained calcium loss and that calculated according to the Livingston model

of Antwerp, namely the UIA, PML and PORT sites, and amounts to around 68–80%. Meanwhile, the calcium loss contribution by calcite dissolution in rain (in equilibrium with atmospheric CO_2) is more significant at the SEA site at 28%. We invoke the marine character and the higher rainfall volumes at this location to be responsible for this outcome. The acid rain effect accounts for approximately 40% of the calcium loss in limestones exposed at the OFF site, and for around 10% at the Antwerp and seaside sites. The obtained results indicate the importance of long-range transport to remote, low-polluted areas and the predominance of local pollution sources in cities and industrial areas. The model-calculated calcium loss approximates the experimentally obtained loss for most of the locations (Fig. 5). However, a very poor model prediction was obtained at the SEA site, with the model largely underestimating the calcium loss. At this point, it should be considered that the physical effects (not included in the model), as for example the salt action disrupting the stones by crystallisation and hydration, can play a decisive role in the decay of limestones at sites near the coast.

The Lipfert model

This model allows only a rough estimate of the three dissolution processes because it uses a fixed number for the clean rain effect (karst effect). Thus, the contribution of this process is similar at all sites. In Fig. 6, the relative contributions of the karst effect, acid rain and dry deposited of SO_2 for the Massangis limestone are shown, obtained by applying the damage function formulated by Lipfert (1989). The results clearly indicate that the karst effect dominates the limestone dissolution at all locations, ranging from 82% at PORT to 97% at SEA. The remaining part of the calcium dissolution is explained by the formation of gypsum. No acid rain effects were observed in the monitoring sites; its contribution was lower than 1%. A comparison between calculated and experimentally obtained stone material loss, expressed as loss per rainfall amount, is shown in Fig. 7. It can be seen that although this model underestimates the stone decay in the highly industrialised area of the PORT, it does give good predictions of material loss at the other sites.

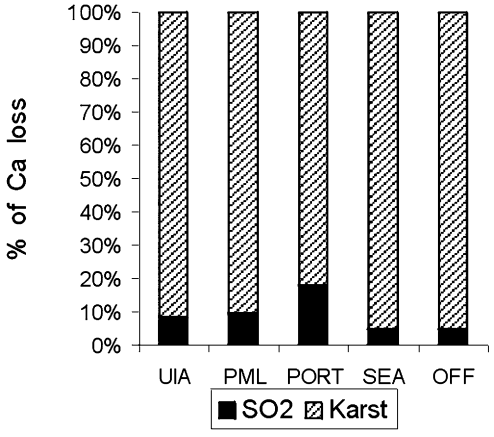

Fig. 6
Relative contributions of the three processes to calcium loss from Massangis stones after the Lipfert model

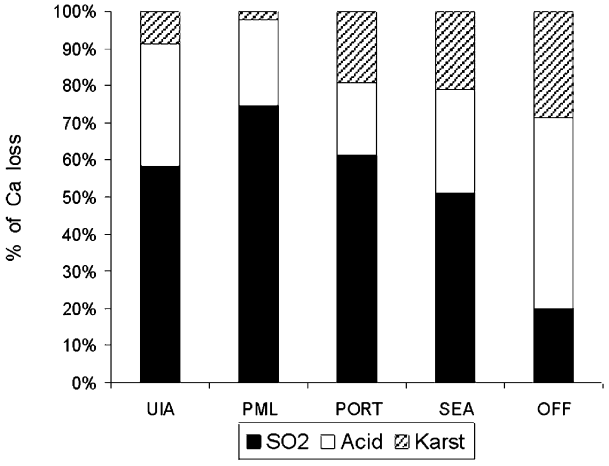

Fig. 8
Relative contributions of the three processes to calcium loss from Massangis stones using the Webb model (K_HK_1 fixed)

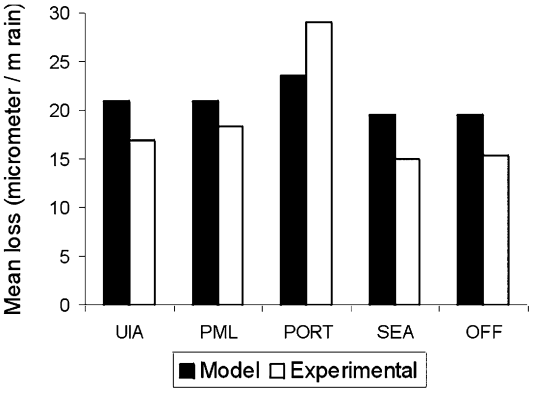

Fig. 7
Comparison of experimentally obtained calcium loss and that calculated according to the Lipfert model

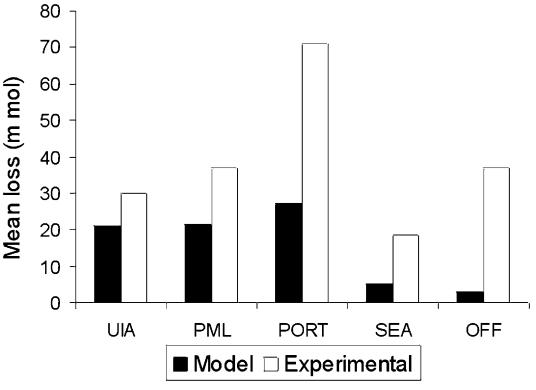

Fig. 9
Comparison of experimentally obtained calcium loss and that calculated (K_HK_1 fixed) according to the Webb model

The Webb model

To adequately describe calcium loss according to the model proposed by Webb and collaborators, some conditions are required: (1) the pH of the run-off water should be at least one unit higher than that of the rain (between 6 and 9), (2) the run-off water should not be enriched in nitrate, ammonium and sea salts, (3) the particulate sulphate deposition should be minimum compared with gaseous dry deposition of SO_2, (4) the granular loss of the stone by physical mechanisms should be very small, and (5) no accumulation of salts at or beneath the stone surface is desirable. These requisites are found for the Massangis limestones exposed at all the monitoring sites in Belgium, which makes it possible to apply this model.

The Webb model can be calculated considering the K_HK_1 product either as a constant or as a product depending on the temperature. The results from both calculation methods are discussed below. The relative contributions of the three dissolution processes to calcium loss, by treating the K_HK_1 product as a constant, are shown in Fig. 8. A predominant contribution of SO_2 dry deposition and the subsequent formation of gypsum is observed for the Massangis stones exposed in the area of Antwerp and at the seaside sites, ranging from around 50 to 75%. The wet acidity effect accounts to calcium loss at approximately 20–50%, as was expected considering the high pH of the total deposition samples. On the other hand, a small contribution of the karst effect was particularly found for the PML site (2–30%). The obtained results are evidence that different decay mechanisms should be expected for the limestones in the five monitoring sites, in view of the different contribution levels of the three dissolution processes to calcium loss. The experimentally obtained losses and the model-calculated calcium losses, taking into account a fixed value for K_HK_1 product, are compared and illustrated in Fig. 9. In all the sites, the model underestimates the calcium loss, especially at the PORT site (as the Lipfert model does), but also at the OFF site. The relative contributions of the three dissolution processes, considering the K_HK_1 product varies with temperature, are shown in Fig. 10. Again, a predominant contribution of SO_2 dry deposition is observed

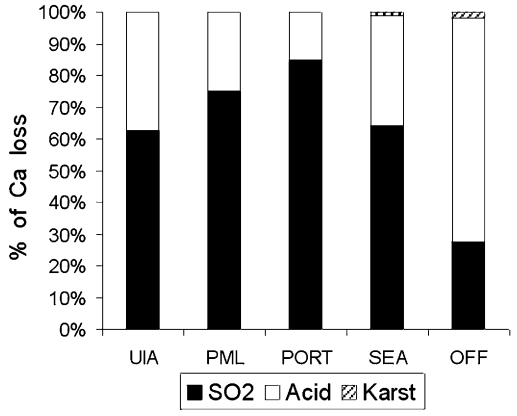

Fig. 10
Relative contributions of the three processes to calcium loss from Massangis stones using the Webb model (K_HK_1 varying with temperature)

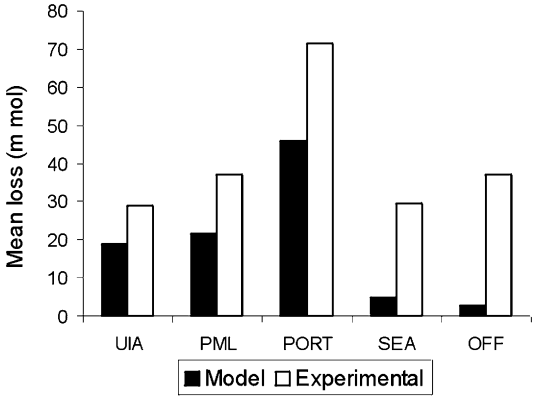

Fig. 11
Comparison of experimentally obtained calcium loss and that calculated (K_HK_1 varying with temperature) according to the Webb model

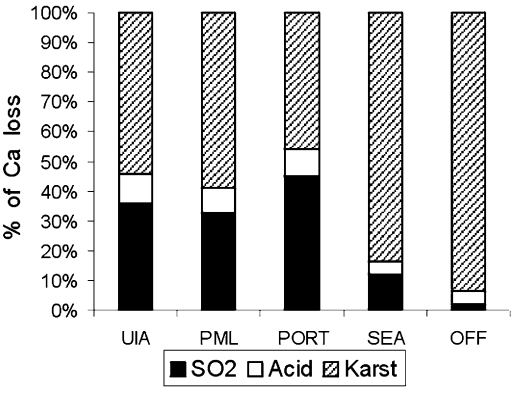

Fig. 12
Relative contributions of the three processes to calcium loss from Massangis stones using the Baedecker model

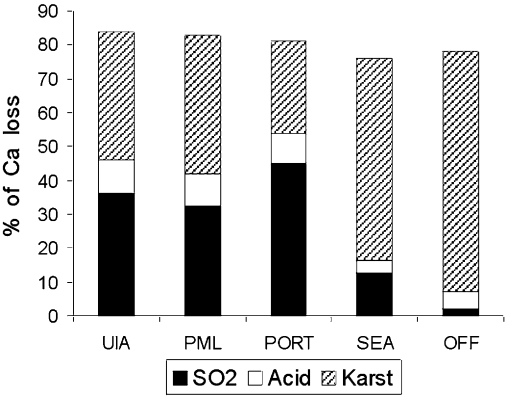

Fig. 13
Relative contributions of the three processes to calcium loss from Massangis stones using the Baedecker model, and allocating experimental HCO_3 loss to the karst effect

for the area of Antwerp and at the seaside site, amounting to 60–85%. The wet acidity effect accounts for 20–70% of the calcium loss, and the contribution of the karst effect is almost negligible. Experimental and calculated calcium losses are compared and represented in Fig. 11. The results show that the model underestimates calcium loss too.

The Baedecker method

In Fig. 12, the contributions of the calculated calcium losses for the Massangis limestones because of rain acidity effect, dry deposition of SO_2 and natural dissolution are shown for the Baedecker model. In the area of Antwerp, around 40–50% of the stone decay by dissolution can be attributed to wet deposition of hydrogen ions, and to dry deposition of sulphur dioxide and nitric acid (these latter are deposited between rain events). The remaining ~50% of the dissolution mechanism is due to the solubility of the limestone in clean rain. At the SEA and OFF sites, the karst effect contributes up to 80%. Similar relative contributions of the dissolution processes to calcium loss are obtained for the Massangis limestones when calculating the karst effect contribution from the measured cumulative excess of HCO_3^- (Fig. 13). The sum of the three dissolution processes is smaller than 100%, which suggests that, in addition to the clean rain, acid rain and dry deposition effects, other processes must be considered for the five monitoring sites. Otherwise, the model does not adequately represent the three processes.

Conclusions

Surface recession rates for the Massangis limestone were calculated from run-off water analysis samples exposed in "microcatchment units", and exposed under different atmospheric conditions at five sites in Belgium. The relative contributions of the karst effect, rain acidity effect and SO_2 dry deposition to calcium loss in the limestones were determined by applying the theoretical calcium dissolution models of Livingston (1986), Lipfert (1989), Webb and

collaborators (1992) and Baedecker and collaborators (1992). The obtained results from the four methods were different, as was expected considering the different parameters that each model takes into account for predicting calcium loss. It was found that, as expected, the Webb model, working with the larger number of variables, gives a better determination of how damage mechanisms contribute to limestone dissolution. Webb's calculations are the most complicated of the referred models. Different results are obtained depending on the calculation method of the K_HK_1 product. Assuming that this product is constant, the karst effect becomes more important than the temperature-dependent calculation. As a consequence, in the latter case, the contribution of the SO_2 deposition effect increases. The relative contribution pattern obtained with the fixed K_HK_1 calculation method is most comparable with Livingston's model results. The Baedecker method is easy to perform, but a low contribution of dry sulphur deposition and acidity effect is encountered. The Lipfert model prevents the accurate determination of the contribution of the three dissolution processes to stone loss because it considers a fixed value for the karst effect. This assumption entails a large contribution of the referred effect at all sites. In addition, each model provides evidence that different damage mechanisms dominate at the selected monitoring sites in Belgium. Nevertheless, the SO_2 effect is the main dissolution process that contributes to calcium loss at all the sites, although mostly in the area of Antwerp (UIA and PML sites), as shown in the Livingston and Webb models. In contrast, the data obtained with the Lipfert and Baedecker model suggest that the most important contribution to stone loss is the karst effect , especially in the non-polluted areas of SEA and OFF. The large acid rain contribution to calcium loss from limestones exposed in the remote, non-polluted sites near the sea and in the hills of southern Belgium emphasises the role of long-range transport.

The experimental data for calcium loss from the Massangis limestone were fitted with four selected theoretical models for calcium dissolution from the literature, and different results were achieved. Following the criterion "the best model is that which predicts the experimental loss the best", the Lipfert model and the Livingston model yield the best results for the five Belgian monitoring sites. Nevertheless, these models underestimated calcium loss, whereas the Webb and Baedecker models overestimated calcium loss. Finally, it should be emphasised that the models are not easy to compare because they use different units. The Livingston model expresses calcium concentration in the run-off water as mol l^{-1}, the Lipfert model expresses the stone loss as μm per meter of rain, the Webb model calculates the net calcium "exchange amount" in mol, and the Baedecker method considers amounts expressed in equivalents. This makes a suitable comparison of the models difficult and causes non-matching of them at first sight.

Acknowledgements This study was financed by the Commission of the European Communities under contract No. EV4V-0052-B (GDF) and STEP CT90-0107.

References

Baedecker PA, Reddy MM, Reiman KJ, Sciammarella CA (1992) Effects of acidic deposition on the erosion of carbonate stone – experimental results from the US National Acid Precipitation Assessment Program (NAPAP). Atmos Environ 26B:147–158

Benarie M (1991) The establishment and use of damage function. In: Baer NS, Sabbioni C, Sors AI (eds) Science, technology and European cultural heritage. Butterworth–Heinemann, Oxford, pp 214–220

Bondarenko I, Treiger B, Van Grieken R, Van Espen P (1995) IDAS, a new Windows based software for multivariate analysis of atmospheric aerosol composition datasets. Proc 9th Int Symp Computer Science for Environmental Protection. Metropolis, Magdeburg, pp 308–315

Butlin RN, Coote AT, Devenish M, Hughes ISC, Hutchens CM, Irwin JG, Lloyd GO, Massey SW, Weeb AH, Yates TJS (1992) Preliminary results from the analysis of stone tablets from the National Materials Exposure Programme (NMEP). Atmos Environ 26B:189–198

Cooper TP (1986) Saving buildings from the weather. Technology Ireland, Dublin

Jeffrey DW, Cooper TP, O'Brien P, Lewis JO, Slattery D, O'Daly G (1985) A test-ring for determining short-term weathering rates of building materials under urban environmental conditions. Effects of air pollution on historic buildings and monuments. Commission of the European Communities, Padua, Italy, pp III83–III93

Kucera V, Fitz S (1995) Direct and indirect air pollution effects on materials including cultural monuments. Water Air Soil Pollut 85:153–165

Lipfert FW (1989) Atmospheric damage to calcareous stones: comparison and reconciliation of recent experimental findings. Atmos Environ 23:415–429

Livingston RA (1986) Evaluation of building deterioration by water runoff. In: Building performance: function, preservation, rehabilitation. American Society for Testing and Materials, Philadelphia, pp 181–188

Livingston RA (1992) Graphical methods for examining the effect of sulphur dioxide on carbonate stones. Proc. 7th Int Congr Deterioration and Conservation of Stone, Laboratorio Nacional de Engenheria Civil, Lisbon, pp 375–386

O'Brien PF, Bell E, Torr TLL, Cooper TP (1995) Stone loss rates at sites around Europe. Sci Total Environ 167:111–121

Reddy MM (1988) Acid rain damage to carbonate stone: a quantitative assessment bases on the aqueous geochemistry of rainfall runoff from stone. Earth Surf Process Landforms 13:335–354

Reddy MM, Sherwood SI, Doe B (1985) Limestone and marble dissolution by acid rain. Proc. 5th Int Congr Deterioration and Conservation of Stone, Lausanne, pp 517–526

Roekens E, Van Grieken R (1989) Rates of air pollution induced surface recession and material loss of a cathedral in Belgium. Atmos Environ 23:271–277

Sherwood SI, Reddy MM (1988) A filed study of pollutant effects on carbonate stone dissolution. Proc 1st Int Symp Engineering Geology of Ancient Works, Monuments and Historical Sites, Greek National Group of IAEG, pp 917–923

Steiger M, Dannecker W (1994) Determination of wet and dry deposition of atmospheric pollutants on building stones by field exposure experiments. Proc. 3rd Int Symp Conservation of Monuments in the Mediterranean Basin, Venice, pp 171–177

Stumm W, Morgan JJ (1970) Aquatic chemistry. Wiley, New York

Sweevers H, Delalieux F, Van Ggrieken R (1998) Weathering of dolomitic sandstone under ambient conditions. Atmos Environ 23:733–748

Torfs K, Van Grieken R (1996) Effect of the stone thickness on run-off water composition and derived damage functions in ambient exposure experiments. Atmos Environ 30:1–8
Tysso V, Esbensen K, Martens H (1987) Unscrambler, an interactive program for multivariate calibration and prediction. Chemometrics Intell Lab Syst 2:239–243
Vleugels G (1992) Weathering of bare and treated limestone under field-exposure conditions in Belgium: study of the runoff water from micro-catchment units. PhD Thesis, University of Antwerp
Vleugels G, Van Grieken R (1995) Suspended matter in run-off water from limestone exposure set up. Sci Total Environ 170:125–132
Webb AH, Bawden RJ, Busby AK, Hopkins JN (1992) Studies on the effects of air pollution on limestone degradation in Great Britain. Atmos Environ 26B:165–181